of iron crossover compounds. The largest bond length change for iron crossover compounds (0.20 A) is reflected in the largest high-spin/low-spin Fe–ligand stretching separation of ~185 cm^{-1} in the Fe[HB(1-pz)$_3$]$_2$ (pz = pyrazolyl) system. A smaller decrease in bond length and change of Fe–N(phen) stretching band position occurs in Fe(phen)$_2$(SCN)$_2$. The Fe(III)–S bond length and stretching band positions are altered even less upon a change from high-spin to low-spin. The similarity of the three high-spin Fe–ligand stretching bands implies that the Fe(III) system does not give as favorable a π overlap as the Fe(II) systems in this low-spin arrangement.

Acknowledgment. This work was supported by the Robert A. Welch Foundation (Grant No. R-483) and the Research Council at Abilene Christian University. We wish to thank the Chemistry Department at the University of Texas at Austin for the use of their Digilab FT-IR.

Registry No. Fe(Et$_2$dtp)$_3$, 18432-76-3; Fe[(pyr)dtc]$_3$, 21288-86-8; Fe(i-Pr$_2$dtc)$_3$, 54181-43-0; Fe(Et$_2$dtc)$_3$, 13963-59-2; Fe(Me$_2$dtc)$_3$, 14484-64-1.

Contribution from the Department of Chemistry,
The University of Kansas, Lawrence, Kansas 66045

Structure of the Gd(fod)$_3$ Adduct of [*N*,*N*′-Ethylenebis(acetylacetone iminato)]nickel(II) in Solution by NMR Spin–Lattice Relaxation Studies

JEAN Y. LEE, DOROTHY A. HANNA, and GROVER W. EVERETT, JR.*

Received September 23, 1980

Gd(fod)$_3$ has a pronounced effect on ^{13}C and ^{1}H NMR spin–lattice relaxation rates of [*N*,*N*′-ethylenebis(acetylacetone iminato)]nickel(II) (I) in chloroform solution. A Gd(fod)$_3$·I adduct is formed which is in rapid equilibrium with its components. The Gd(III) ion is assumed to bind to both oxygens of I with normal Gd–O bond lengths, and the position of Gd(III) relative to I is determined from analysis of paramagnetic contributions to the relaxation rates of two carbon atoms. The Gd(III) ion is located at a point ~1.8 Å out of the plane of I. Distances from Gd(III) to the other carbon atoms and to the protons are calculated from the appropriate NMR relaxation rates. These distances are compared with those determined with the use of crystallographic data for I and by assuming that Gd(III) is located correctly by the NMR data. The agreement is within the limits of error in all cases, thus supporting assumptions made in devising the model.

Introduction

The theory of nuclear relaxation in the presence of paramagnetic ions was developed in the 1950's by Solomon, Bloembergen, and other,[1-5] and during the following two decades paramagnetic ion enhanced nuclear relaxation data has been applied numerous times to obtain structural information on enzymes in the solution phase.[6-9] Several comprehensive reviews of the theory and applications of this method are available.[10-12]

Up to the present time, there have been relatively few applications of NMR relaxation enhancement techniques to smaller molecules. Structural information has been obtained by using selected paramagnetic ions as relaxation probes for borneols,[13] ATP,[14] AMP,[15] histidine,[16,17] *N*-acetyl-3-nitrotyrosine,[18] sarcosine,[19] catecholamines,[20] an iron(III) porphyrin,[21] and a thiocyanate complex of Gd(III).[22]

A paper by Lindoy and Moody[23] in 1977 described interactions of the lanthanide shift reagents Eu(fod)$_3$ and Pr(fod)$_3$ (where fod is the anion of CF$_3$CF$_2$CF$_2$COCH$_2$COC(CH$_3$)$_3$) with diamagnetic, planar complexes such as I. The pattern of observed ^{1}H and ^{13}C isotropic shifts strongly indicates that the oxygen atoms of I are bound to the lanthanide ion in a bidentate manner as shown in II. Plots of isotropic shifts vs. the mole ratio of Ln(fod)$_3$:I show that the stoichiometry of the adduct is 1:1.

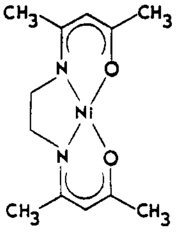

I

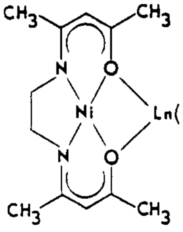

II

The proposed structure of the adduct is in accord with the known tendency of lanthanide ions in shift reagents to expand their coordination numbers from 6 to 8.[24] It is also consistent

---

(1) Solomon, I. *Phys. Rev.* **1955**, *99*, 559–565.
(2) Bloembergen, N. *J. Chem. Phys.* **1957**, *27*, 572–573.
(3) Codrington, R. S.; Bloembergen, N. *J. Chem. Phys.* **1958**, *29*, 600–604.
(4) Bernheim, R. A.; Brown, T. H.; Gutowski, H. S.; Woessner, D. E. *J. Chem. Phys.* **1959**, *30*, 950–956.
(5) Swift, T. J.; Connick, R. E. *J. Chem. Phys.* **1962**, *37*, 307–320.
(6) Mildvan, A. S.; Cohn, M. *Adv. Enzymol. Relat. Areas Mol. Biol.* **1970**, *33*, 1–70.
(7) Cohn, M.; Reuben, J. *Acc. Chem. Res.* **1971**, *4*, 214–222.
(8) Mildvan, A. S. *Acc. Chem. Res.* **1977**, *10*, 246–252.
(9) Mildvan, A. S.; Gupta, R. K. *Methods Enzymol.* **1978**, *49*, (*Part G*), 332–359.
(10) Dwek, R. A.; Williams, R. J. P.; Xavier, A. V. In "Metal Ions in Biological Systems"; Siegel, H., Ed.; Marcel Dekker: New York, 1974; Vol. 4.
(11) James, T. L. "Nuclear Magnetic Resonance in Biochemistry"; Academic Press: New York, 1975.
(12) Dobson, C. M.; Levine, B. A. In "New Techniques in Biophysics and Cell Biology"; Pain, R. H., Smith, B. J., Eds.; Wiley: New York, 1976; Vol. 3.
(13) Levy, G. C.; Komoroski, R. A. *J. Am. Chem. Soc.* **1974**, *96*, 678–681.
(14) Lam, Y. F.; Kuntz, G. P. P.; Kotowycz, G. *J. Am. Chem. Soc.* **1974**, *96*, 1834–1839.
(15) Fan, S.; Storer, A. C.; Hammes, G. *J. Am. Chem. Soc.* **1977**, *99*, 8293–8298.
(16) Led, J. J.; Grant D. M. *J. Am. Chem. Soc.* **1975**, *97*, 6962–6970.
(17) Led, J. J.; Grant, D. M. *J. Am. Chem. Soc.* **1977**, *99*, 5845–5858.
(18) Marinetti, T. D.; Snyder, G. H.; Sykes, B. D. *J. Am. Chem. Soc.* **1975**, *97*, 6562–6570.
(19) Elgavish, G. A.; Reuben, J. *J. Am. Chem. Soc.* **1978**, *100*, 3617–3619.
(20) Granot, J. *J. Am. Chem. Soc.* **1978**, *100*, 2886–2891.
(21) Viscio, D. B.; LaMar, G. N. *J. Am. Chem. Soc.* **1978**, *100*, 8092–8096.
(22) Musikas, C.; Cuillerdier, C.; Chachaty, C. *Inorg. Chem.* **1978**, *17*, 3610–3615.
(23) Lindoy, L. F.; Moody, W. E. *J. Am. Chem. Soc.* **1977**, *99*, 5863–5870.

0020-1669/81/1320-2004$01.25/0

with the structure, determined by crystallography, of the $Na^+ClO_4^-$ adduct of I where the Na^+ ion is bound to the two oxygens of each of two nickel complexes.[25] Furthermore, oxygen-bound adducts of this type with metal cations are well-known for the closely related complexes of salicylaldimines.[26]

The NMR signals of I observed in the presence of Ln(fod)$_3$ are averages of those of I and the adduct II. A study of the dependence of the ^1H NMR line widths and isotropic shifts on the shift reagent:substrate ratio showed that the lifetime of the adduct for Ln = Eu^{3+} is about 2×10^{-5} s (fast exchange).[27]

This series of complexes appears to be ideally suited for solution structural studies using "relaxation reagents" such as Gd(fod)$_3$. The binding site, stoichiometry, and lifetime of the adduct are expected to be the same for Gd(fod)$_3$ as for Eu(fod)$_3$. Structural parameters of complexes of type I in the solid state are well documented by crystallographic studies.[28-34] In this paper, ^1H and ^{13}C relaxation data for the Gd(fod)$_3$ adduct of substrate I are used to determine the location of bound Gd(III) in the adduct and distances, *r*, from the Gd(III) ion to the nuclei of I. These *r* values are compared with those calculated with use of the crystallographic coordinates of I.

Theory

Paramagnetic ions such as Mn^{2+} and Gd^{3+} which have several unpaired electrons, isotropic *g* values, and relatively long electron spin relaxation times are extremely efficient at enhancing relaxation rates of nearby nuclei. An increase in the transverse (spin–spin) relaxation rate, T_2^{-1}, shows up as NMR signal broadening. The selectivity in signal broadening can be used qualitatively to locate the binding site of a paramagnetic ion. However, as discussed previously,[36,37] this method is of questionable value for quantitative structural determinations. In principle, fairly accurate structural information can be derived from the effect of paramagnetic ions on T_1^{-1}, the longitudinal (or spin–lattice) relaxation rate.[10-12]

The rate of spin–lattice relaxation of a nucleus in a molecule bound to a paramagnetic ion is given by the Solomon–Bloembergen equation (eq 1).[1-5] Here *r* is the length of the vector from the paramagnetic ion to the nucleus, τ_c and τ_e are correlation times for dipolar and contact interactions, respectively, between the ion and the nucleus, and *A* is the electron-nuclear contact coupling constant. The other symbols have their usual meanings.[10-12] The first term on the right in eq 1 expresses the dipolar contribution to the relaxation rate. The second term gives the contribution from contact interactions, and it can be shown that if $\omega_S^2\tau_e^2 >> 1$, this term will be negligibly small. This is generally the case in the magnetic fields of most NMR spectrometers for ions such as Mn^{2+} or Gd^{3+}. Thus if T_{1M}^{-1} can be extracted from experimental relaxation rate data, structural information is available through the r^{-6} dependence of the dipolar term of eq 1.

$$\frac{1}{T_{1M}} = \frac{2}{15}\frac{\gamma_I^2 g^2 S(S+1)\beta^2}{r^6}\left[\frac{3\tau_c}{1+\omega_I^2\tau_c^2} + \frac{7\tau_c}{1+\omega_S^2\tau_c^2}\right] + \frac{2}{3}S(S+1)\left[\frac{A}{\hbar}\right]^2\left[\frac{\tau_e}{1+\omega_S^2\tau_e^2}\right] \quad (1)$$

In practice, two approaches to the use of eq 1 have developed. If the remaining quantities in the dipolar term are known, *r*'s may be obtained directly from T_{1M}^{-1} data. The principal drawback to this approach is that τ_c cannot always be determined accurately. The other approach is to assume that τ_c will be constant for all nuclei in the ion-substrate complex.[35] Then $T_{1M}^{-1} = Kr^{-6}$ for nuclei of the same kind. The constant *K* need not be known if *ratios* of T_{1M}^{-1}'s are used to determine *ratios* of *r*'s (eq 2).

$$T_{1M_i}^{-1}/T_{1M_j}^{-1} = r_j^6/r_i^6 \quad (2)$$

In most experiments involving paramagnetic relaxation agents such as Mn^{2+} or Gd^{3+}, the ion:substrate ratio must be very small or T_1 measurements will be impossible due to severe signal broadening. Under conditions of fast exchange, the observed relaxation rate, T_{1obsd}^{-1} is given by eq 3.[10-12] Here

$$\frac{1}{T_{1obsd}} = \frac{1-P_M}{T_{1f}} + \frac{P_M}{T_{1M}+\tau_M} + \frac{1}{T_{1os}} \quad (3)$$

P_M is the mole fraction of ion-bound substrate, T_{1f}^{-1} is the relaxation rate of the nucleus in the ion-free substrate, τ_M is the lifetime of the complex, and T_{1os}^{-1} is the contribution from "outer sphere" relaxation. The latter arises from the influence of ions not directly bound to the substrate.

Generally, $P_M << 1$, and the *paramagnetic* contribution to the observed relaxation rate is defined by eq 4. T_{1f}^{-1} is

$$\frac{1}{T_{1P}} = \frac{1}{T_{1obsd}} - \frac{1}{T_{1f}} = \frac{P_M}{T_{1M}+\tau_M} + \frac{1}{T_{1os}} \quad (4)$$

obtained from relaxation time studies of the substrate alone or of a suitable diamagnetic complex, and T_{1os}^{-1} may be estimated from measured paramagnetic contributions to relaxation rates of "inert" molecules such as tetramethylsilane, which do not bind to the inner coordination sphere of the metal ion.

If it can be demonstrated that $T_{1M} >> \tau_M$ (rapid exchange) observed relaxation rate data can be used in eq 4 to obtain $P_M T_{1M}^{-1}$. The value of P_M need not be known in order to obtain *ratios* of *r*'s, since $T_{1P}^{-1} = P_M T_{1M}^{-1}$, and from eq 2, eq 5 can be derived.

$$\frac{T_{1P_i}^{-1}}{T_{1P_j}^{-1}} = \frac{r_j^6}{r_i^6} \quad (5)$$

Experimental Section

Instrumentation. All NMR experiments were carried out on a Bruker WP-80 Fourier transform spectrometer equipped with a Bruker ASP-2000 computer and operating at 80.0 MHz for protons and 20.1 MHz for carbon-13. Quadrature phase detection was used in all cases, and accumulated fid's were stored on hard magnetic disks. Sample temperatures were monitored with a Bruker B-VT-1000 temperature controller.

Microprograms written to direct computer acquisition of T_1 data were tested with the use of dioxane/D_2O samples, and T_1 values

---

(24) Sievers, R. E., Ed. "Nuclear Magnetic Resonance Shift Reagents"; Academic Press: New York, 1973.

(25) Armstrong, L. G.; Lip, H. C.; Lindoy, L. F.; McPartlin, M.; Tasker, P. A. *J. Chem. Soc., Dalton Trans.* **1977**, 1771–1774.

(26) Sinn, E.; Harris, C. M. *Coord. Chem. Rev.* **1969**, *4*, 391–422.

(27) Beattie, J. K.; Lindoy, L. F.; Moody, W. E. *Inorg. Chem.* **1976**, *15*, 3170–3172.

(28) Cariati, F.; Morazzoni, F.; Busetto, C.; Del Piero, G.; Zazzetta, A. *J. Chem. Soc., Dalton Trans.* **1976**, 342–347.

(29) Brückner, S.; Calligaris, M.; Nardin, G.; Randaccio, L. *Inorg. Chim. Acta* **1968**, *2*, 386–390.

(30) Curtis, N. F.; Baker, E. N.; Hall, D.; Waters, T. N. *Chem. Commun.* **1966**, 675–676.

(31) Hall, D.; Rae, A. D.; Waters, T. N. *J. Chem. Soc.* **1963**, 5897–5901.

(32) Clark, R. G.; Hall, D.; Waters, T. N. *J. Chem. Soc. A* **1968**, 223–226; **1969**, 823–829.

(33) Lindoy, L. F.; Moody, W. E.; Taylor, D. *Inorg. Chem.* **1977**, *16*, 1962–1968.

(34) Scaringe, R. P.; Hodgson, D. J. *Inorg. Chem.* **1976**, *15*, 1193–1199.

(35) This assumption is not rigorously valid when τ_c is dominated by the rotational correlation time, τ_r, and molecular rotation is not isotropic or the motional properties of individual groups differ from those of the molecule as a whole.

(36) Esperson, W. G.; Martin, R. B. *J. Phys. Chem.* **1976**, *80*, 161–164.

(37) Esperson, W. G.; Martin, R. B. *J. Am. Chem. Soc.* **1976**, *98*, 40–44.

obtained were in good agreement with published values.[38]

Calibration of the 180°/90° pulse width was checked frequently with the use of dioxane in D_2O for ^{13}C and Me_4Si in $CDCl_3$ for protons. During calibrations, the pulse was set close to the signal in each case, and plots of normalized signal intensities vs. pulse width were extrapolated to zero intensity to determine the 180° pulse width. A 90° pulse requires 9.7 μs with an apparent variation ≤ 0.4 μs over a 2-year period. The H_1 pulse power for both ^1H and ^{13}C probeheads was found to be more than adequate to cover the entire range of chemical shifts, e.g., for ^{13}C, H_1 is $\sim$24 G which corresponds to more than 1000 ppm. Examination of the pulse profile for the ^{13}C probe using a high-frequency storage oscilloscope showed the pulse to have a rapid rise time and sharp cutoff. This experiment also provided a check on the calibration of the pulse width circuitry of the spectrometer (actual pulse width in μs vs. computer input in μs).[38]

Relaxation Time Measurements. The inversion-recovery method $(5T_1\text{–}180°\text{–}\tau\text{–}90°)_n$ with 8K data points for 1000-Hz sweep width was used for all proton work. Samples were contained in spherical microcells approximately 4 mm in diameter. These were positioned inside cylindrical samples tubes (5-mm o.d.) so that the spherical chamber was centered in the transmitter coil of the spectrometer during NMR experiments. This was found to eliminate most of the problems associated with inhomogeneity of the H_1 pulse (by comparison of absolute values of normalized signal intensities after 90° and 270° pulses). The spherical chamber was surrounded by chloroform or D_2O in each case.

Carbon-13 data for samples containing $Gd(fod)_3$ were collected with the use of a time-saving modification of the inversion-recovery method proposed by Canet, Levy, and Peat, referred to as FIRFT.[39] The sequence is $(T\text{–}180°\text{–}\tau\text{–}90°)_n$ where $T < 5T_1$ and the first FID is not retained. Generally, 1000 fid's were accumulated and stored on a hard disk for each τ. Some ^{13}C T_1's were rather long (>10 s) when samples contained $La(fod)_3$, and data acquisition for these nuclei proved to be more efficient with the use of the progressive saturation method $(90°\text{–}\tau)_n$. These samples were saturated with N_2 to remove O_2 prior to relaxation time measurements. Data for other carbon nuclei in samples containing $La(fod)_3$ were collected by the FIRFT method. All ^{13}C spectra were run under conditions of proton broad-band decoupling with use of 16K data points over a 5000-Hz spectral width. Samples were contained in cylindrical inserts, approximately 8 mm in diameter by 10 mm in length, which were positioned inside 10-mm o.d. cylindrical sample tubes so as to confine the sample to the dimensions of the transmitter coil.

During data acquisition, short and long delays (τ) were placed in random order in most cases to avoid systematic errors.[40] At least two fully relaxed spectra ($\tau > 5T_1$) were obtained during runs lasting more than 1 h in order to provide a check on changes in H_0 homogeneity. Further compensation for small changes in H_0 homogeneity with time was made by applying an exponential multiplication factor[38,40] to the accumulated fid's, corresponding to line broadening of 5 Hz for ^{13}C and 2 Hz for protons. Temperatures were maintained constant to within ±1° in all cases.

Fortran programs designed to compare normalized signal intensities, to draw plots of $\ln (M_0 - M_\tau)$ vs. τ, and to determine T_1's by a linear least-squares routine were run on a Honeywell 66/60 computer located on campus. In most cases, 10–15 data points, including points on both sides of the null position, were used in the least-squares calculations.

Sample Preparation. So that problems due to adventitious paramagnetic ions could be avoided, all solutions and solvents were prevented from coming into contact with metal objects such as syringe needles, vortex rods, spatulas, etc., and all glassware was soaked in an EDTA solution prior to use. Stock solutions of known concentrations of $Gd(fod)_3$ and $La(fod)_3$ in $CDCl_3$ were prepared. Measured volumes of these stock solutions were added to weighed amounts of substrate I, and $CDCl_3$ was added until the concentration of I was in the range 0.19–0.24 M. The $Gd(fod)_3$:I mole ratios were in the range 10^{-2}–10^{-3} for both ^{13}C and ^1H experiments. A small amount of Me_4Si was added in most cases, and the solutions were transferred to the above-described sample tubes with use of glass pipets.

The Ni(II) complex, I, was prepared by a published method.[33]

Results and Discussion

As outlined in the Theory section, in order to relate experimental relaxation rates to Gd–nuclear distances with the use of the Solomon–Bloembergen equation, it must be demonstrated that $\tau_M << T_{1M}$ (eq 4, rapid exchange).

In an earlier study of the adduct of I with $Eu(fod)_3$, Beattie, Lindoy, and Moody[27] found $\tau_M \approx 2 \times 10^{-5}$ s, with use of rigorously dried $CDCl_3$ as solvent, or $\approx 6 \times 10^{-6}$ s with use of $CDCl_3$ as purchased. In the present study, $CDCl_3$ was used as supplied, and it is reasonable to assume τ_M is of the order of 10^{-5} s for the $Gd(fod)_3$ adduct. With use of the shortest experimental ^1H and ^{13}C T_{1P} values obtained for I in the presence of $Gd(fod)_3$ (0.0555 and 0.113 s, respectively) and P_M values[41] of 7×10^{-3} (^{13}C) and 4×10^{-3} (^1H) in eq 4, it is clear that the *shortest* T_{1M} values are between 1 and 2 orders of magnitude larger than τ_M for both protons and carbons.

Further support for rapid exchange is obtained from the temperature dependence of proton T_{2p}'s for complex I in the presence of $Gd(fod)_3$. Proton spectra of I with a $Gd(fod)_3$:substrate mole ratio $\approx 4 \times 10^{-3}$ were recorded at temperatures in the range 273–325 K. Similarly, spectra of I in the presence of $La(fod)_3$ were recorded at the same temperatures. T_{2p}^{-1} values, determined from line-width measurements,[42] were plotted against K^{-1}. In all cases positive slopes were found, indicating that rapid exchange conditions are maintained for transverse relaxation,[10,11] i.e., $T_{2M} >> \tau_M$. Since one expects $T_{2M} < T_{1M}$, it follows that $\tau_M << T_{1M}$. These experiments indicate that at temperatures employed in this work for spin–lattice relaxation time measurements, the fast exchange condition holds for protons. Since T_{1M}'s for carbons are larger than those for protons, τ_M in eq 4 will also be negligible for ^{13}C data.

Carbon-13 NMR Experiments. The $Gd(fod)_3$:I mole ratios were chosen empirically so as to cause significant enhancement in spin–lattice relaxation without severe signal broadening. Partially relaxed ^{13}C spectra for sample B are shown in Figure 1 with signal assignments given in the fully relaxed spectrum. The numbering scheme is defined in Figure 2.

Paramagnetic contributions (T_{1P}^{-1}) to the observed spin–lattice relaxation rates were determined by using eq 4 where T_{1f}^{-1} values are assumed to be adequately represented by the observed relaxation rates in the presence of $La(fod)_3$. So that T_{1os}^{-1} could be estimated, ^{13}C spin–lattice relaxation rates of cyclohexane and Me_4Si in solutions containing $Gd(fod)_3$ and I were compared with those measured in solutions containing $La(fod)_3$ and I. The difference in observed T_1^{-1} values for these inert molecules in the paramagnetic and diamagnetic samples is assumed to represent T_{1os}^{-1}. Values found are 0.025 s^{-1} (cyclohexane) and 0.028 s^{-1} (Me_4Si). Accordingly, an outer-sphere correction of 0.03 s^{-1} was made on all data.

Table I contains the ^{13}C relaxation data after T_{1f}^{-1} and T_{1os}^{-1} corrections. These are referred to hereafter "T_{1P}^{-1}" data. The observed decrease in T_{1P}^{-1} for a given carbon from samples A–E results from the decrease in mole fraction, P_M, of $Gd(fod)_3$ among these samples. Under conditions of fast exchange, T_{1P}^{-1} values could be plotted as a function of P_M in order to obtain an average T_{1M}^{-1} for each carbon atom (eq 4). These T_{1M}^{-1} values could then be used in eq 2 to obtain distance ratios. However, this procedure requires that P_M values be accurately known and offers no advantage when distance ratios are sought. Thus we have chosen to determine

---

[38] Armitage, I. M.; Huber, H.; Live, D. H.; Pearson, H.; Roberts, J. D. *J. Magn. Reson.* **1974**, *15*, 142–149.

[39] Canet, D.; Levy, G. C.; Peat, I. R. *J. Magn. Reson.* **1975**, *18*, 199–204.

[40] Levy, G. C.; Peat, I. R. *J. Magn. Reson.* **1975**, *18*, 500–521.

[41] The assumption is made here that the mole fraction of bound ligand, P_M, is the same as the $Gd(fod)_3$:I mole ratio. This will be true where K_f for the adduct is large and the $Gd(fod)_3$:I ratio is small. A K_f of $\sim 10^3$ was found[27] for the $Eu(fod)_3$ adduct of I, and it is reasonable to assume a similar K_f for the $Gd(fod)_3$ adduct.

[42] Contributions to the line width arising from magnetic field inhomogeneities should effectively be cancelled when data from the two solutions are compared.

Table I. Paramagnetic Contributions to Carbon-13 Spin-Lattice Relaxation Rates for I in the Presence of Gd(fod)$_3$

			T_{1P}^{-1}, s^{-1} [a,b]				
position	no.[c]	shift[d]	A	B	C	D	E
$CH_3(O)$	1	24.4	4.64 (30)	3.38 (19)	1.48 (10)	1.25 (21)	0.718 (53)
C=O	2	176.9	8.86 (61)	7.36 (87)	2.18 (17)	1.93 (27)	1.31 (14)
CH	3	99.6	1.68 (19)	1.28 (10)	0.545 (100)	0.573 (150)	0.207 (67)
C=N	4	164.7	0.960 (54)	0.486 (47)	*e*	0.346 (72)	0.157 (31)
$CH_3(N)$	5	21.1	0.259 (28)	0.167 (32)	*e*	0.0255 (215)	0.0116 (270)
CH_2	6	53.2	0.743 (75)	0.518 (77)	*e*	0.182 (51)	0.184 (49)

[a] Observed relaxation rates less T_{1f}^{-1} and T_{1OS}^{-1}. Rates observed in the presence of La(fod)$_3$ are 0.312 (15), 0.0647 (151), 0.612 (34), 0.0587 (126), 0.2693 (104), and 0.488 (30) s^{-1} for C(1)–C(6), respectively. A value of 0.030 s^{-1} was used for T_{1OS}^{-1} in each case. Sample temperatures are 308 ± 1 K in all cases. [b] Errors in the least significant digits are given in parentheses. [c] Numbering system used in Figure 2. [d] Chemical shift in ppm from Me_4Si. [e] Insufficient number of data points at long τ's to determine these values.

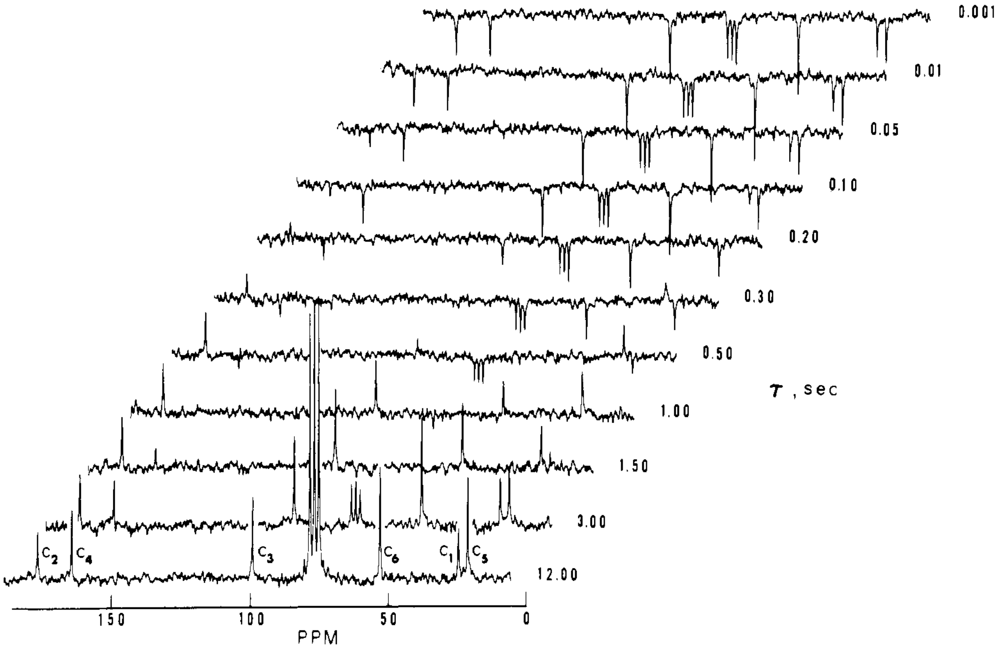

Figure 1. Partially relaxed ^{13}C NMR spectra of I in the presence of Gd(fod)$_3$ is chloroform-*d* solution (sample B). Spectra were obtained with the use of the fast inversion-recovery method.

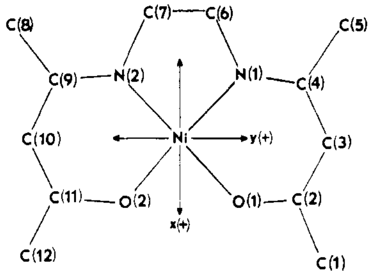

Figure 2. Diagram of substrate I showing the numbering scheme and coordinate system used in specifying atomic positions.

distance ratios directly for each sample using eq 5. Ratios of T_{1P}^{-1} values for any two carbons are fairly consistent from sample to sample, indicating a constant stoichiometry and structure for the adduct over a nearly twofold change in Gd(fod)$_3$ concentration.

T_{1f}^{-1} makes an appreciable contribution to $T_{1\text{obsd}}^{-1}$ for carbons 5 and 6 which are most distant from the oxygens of I (where Gd(fod)$_3$ is presumed to be bound). Errors in T_{1P}^{-1} are relatively large in these cases. On the other hand, for carbons 1 and 2, relaxation enhancement by Gd(III) is sufficiently large that relative errors in T_{1P}^{-1} are minimized. For this reason spin–lattice relaxation data for carbons 1 and 2 are used to find the position of bound Gd(III) relative to substrate I in the Gd(fod)$_3$·I adduct.

It was assumed initially that the Gd ion is bound equally to both oxygens of I at a Gd–O distance of 2.45 Å, a value reported to be the average of values from several crystallographic studies of lanthanide substrate complexes.[24,43] Thus Gd should be located on an arc 2.45 Å from each O. Crystallographic coordinates for atoms of I, reported by Cariati et al.,[28] were converted to a Cartesian coordinate system calibrated in Å with Ni at the origin. The carbon atoms of I are almost entirely in the *xy* plane, and the arc containing Gd is in the *xz* plane in this coordinate system (see Figure 2). A program was written which calculates ratios of distances from carbons 1 and 2 to Gd, $r(2)/r(1)$, at various points on the arc,[44] with use of the crystallographic data, and compares these ratios with the ratio obtained from T_{1P}^{-1} data by using eq 5. The Gd(III) ion is assumed to be located at the coordinates where the best agreement between the calculated and experimental ratios is obtained.

Table II gives the coordinates of Gd in the *xz* plane determined in the above manner. Also presented are Gd–carbon distance ratios, $r(2)/r(i)$, determined from the T_{1P}^{-1} data by using eq 5. Three columns of data appear in the table: (1) data averaged over all five samples; (2) data averaged over

---

(43) In a very recent crystal structure determination of the DMF adduct of Eu(thd)$_3$, the Eu–O(DMF) distance was found to be 2.471 (24) Å: Cunningham, J. A.; Sievers, R. E. *Inorg. Chem.* **1980**, *19*, 595–604.

(44) During these calculations, Gd was placed at points along the arc corresponding to increments of 0.001 Å in the *x* coordinate.

Table II

Gd–Carbon Distance Ratios and Structural Data for the $Gd(fod)_3 \cdot I$ Adduct

dist ratios[a]	av of samples A–E[b]	av of samples A and B[b]	sample A only[b]
$r(2)/r(1)$	0.910 (29)	0.888 (23)	0.898 (20)
$r(2)/r(3)$	0.770 (38)	0.753 (24)	0.758 (23)
$r(2)/r(4)$	0.695 (29)	0.663 (18)	0.690 (14)
$r(2)/r(5)$	0.507 (76)	0.544 (22)	0.555 (16)
$r(2)/r(6)$	0.675 (34)	0.653 (23)	0.662 (19)
coords of Gd using $r(2)/r(1)$,[c] Å	$x = 2.72$ (34) $z = 1.65$ (30)	$x = 2.47$ (27) $z = 1.83$ (18)	$x = 2.58$ (24) $z = 1.75$ (17)
Gd–C(2), dist, $r(2)$, Å	3.34 (28)	3.34 (19)	3.33 (17)
Comparison of Gd–Carbon Distances,[d] Å			
Gd–C(3) NMR	4.34 (58)	4.44 (39)	4.39 (36)
X-ray	4.46 (30)	4.39 (22)	4.41 (19)
Gd–C(4) NMR	4.81 (60)	5.04 (42)	4.83 (34)
X-ray	4.95 (36)	4.82 (27)	4.88 (24)
Gd–C(5) NMR	6.59 (154)	6.13 (60)	6.00 (48)
X-ray	6.41 (33)	6.26 (26)	6.32 (22)
Gd–C(6) NMR	4.95 (66)	5.11 (48)	5.03 (40)
X-ray	5.69 (41)	5.51 (31)	5.59 (27)

[a] Ratio of distances from Gd to carbon atoms C(2) and C(*i*), $r(2)/r(i)$. See numbering system in Figure 2. [b] Errors in the least significant digits are given in parentheses. These are cumulative errors originating from the errors in $T_{1\text{obsd}}^{-1}$. [c] Gd constrained to the *xz* plane (Figure 2) with Gd–O bond lengths of 2.45 Å. [d] NMR distances were determined by using the distance ratios and $r(2)$. "X-ray" distances were determined by using the experimental Gd coordinates and crystallographic positions for carbon atoms in the coordinate system shown in Figure 2.

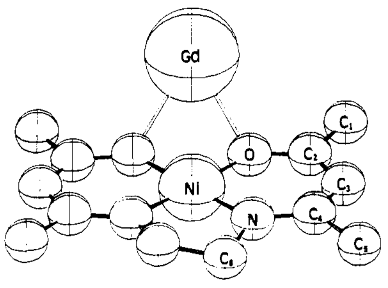

Figure 3. ORTEP plot of I showing the Gd ion bound at the coordinates found for sample A. Atomic sizes are proportional to their covalent radii.

samples A and B (believed to be the most accurate as a result of relatively large T_{1P}^{-1} values); (3) data for sample A alone. It is apparent that the Gd ion is significantly out of the plane of I (see Figure 3). This is not without precedent. A crystallographic study of the $NaClO_4$ adduct of I shows Na^+ is bound to four oxygens from two molecules of I and to two perchlorate oxygens.[25] The Na^+ ion is out of the planes of both nickel complexes. Also, an example of out-of-plane coordination to oxygens of a tetradentate salicylaldimine complex of Cu(II) was reported recently.[45] In the present case, out-of-plane coordination is probably the result of steric interactions between the methyl groups of I and the fod ligands.

Having located the Gd ion using T_{1P}^{-1} data for carbons 1 and 2, we test the model further by comparing distances from Gd to the remaining carbons, as determined by NMR data, with distances calculated with the use of the crystallographic coordinates. So that the "NMR" distances could be determined, the Gd–C(2) distances shown in Table II were used in eq 5 with experimental ratios $T_{1P}^{-1}(i)/T_{1P}^{-1}(2)$. The *r* values so obtained by using (a) data averaged over all five samples, (b) data averaged over samples A and B, and (c) data from sample A alone are compared in Table II.

In all cases the NMR and "X-ray" distances agree within the limits of error, thus supporting the basic assumptions made in devising the model. The agreement is not improved by allowing longer or shorter Gd–O bond lengths. The errors originate in the T_1 experiments and can arise from a variety of sources. Techniques designed to reduce experimental error have been described,[38,40] and these were used insofar as possible in collecting the data (see Experimental Section). The error limits shown in Table I were obtained from analysis of the ln $(M_0 - M_\tau)$ vs. τ data by using Student's *t* distribution with a 95% confidence interval.[46]

There are several other potential sources of error in the Gd–carbon distances. Delocalization of electron spin from Gd to the substrate may occur. Even in the absence of significant scalar contributions to T_{1M}, spin delocalization could result in one or more substrate atoms as *local* paramagnetic relaxers, thereby complicating the relationship between T_{1M} and the Gd–carbon distances. This effect is expected to be most pronounced for the carbons in the conjugated chelate ring of the substrate. However, the general agreement between NMR and "X-ray" distances for C(3) and C(4), which were not used to locate Gd, implies little spin delocalization. This is supported by the fact that observed isotropic shifts are very small ($\leq$0.1 ppm).

Equations 2 and 5 assume the correlation time, τ_c, is the same for all nuclei. If τ_c is dominated by τ_r, and if molecular reorientation is not isotropic or if the motional properties of certain groups differ from that of the molecule as a whole, errors in *r* values will result. It is likely, but not certain, that τ_r dominates τ_c here since published values of τ_s for Gd(III) in a variety of environments agree that $\tau_s \geq 10^{-10}$ s.[18,22,47–48,52] The fact that the Gd–carbon distances determined from T_1 data agree within the limits of error with those calculated from crystallographic coordinates implies that errors arising from differences in τ_c are relatively small. Note that since $r \propto (\tau_c)^{1/6}$, uncertainties in τ_c will result in much smaller uncertainties in *r*.

Finally, it should be pointed out that distances determined by relaxation enhancement methods may, under fast-exchange conditions, represent averages of several distinct adduct species.[49] For substrate I, however, conformational changes are expected to be small and Gd binding can occur only at oxygen. The only reasonable adduct structure is that depicted in Figure 3. Other structures such as one in which Gd binds to only one oxygen are unrealistic from steric considerations.

Proton NMR Experiments. Proton NMR spectra of I in the presence of $Gd(fod)_3$ or $La(fod)_3$, at a Ln:I mole ratio of $\sim 4 \times 10^{-3}$, show only three signals attributable to protons of I. Signals arising from the $C(1)H_3$ and $C(5)H_3$ protons are accidentally coincident at 1.87 ppm. The presence of two signals at this frequency having different spin–lattice relaxation times is clearly evident in the partially relaxed spectra. No attempts were made initially to measure relaxation times of these protons.

Plots of ln $(M_0 - M_\tau)$ vs. τ are linear for the C(3)H and $C(6)H_2$ signals. T_{1P}^{-1} data for these protons are given in Table III, where where F and G are two independent samples. Outer-sphere corrections were estimated from Me_4Si and

---

(45) Leslie, K. A.; Drago, R. S.; Stucky, G. D.; Kitko, D. J.; Breese, J. A. *Inorg. Chem.* **1979**, *18*, 1885–1891.

(46) Hoel, P. G. "Introduction to Mathematical Statistics"; Wiley: New York, 1971.

(47) Reuben, J. *J. Phys. Chem.* **1971**, 75, 3164–3167.

(48) Lenkinski, R. E.; Dallas, J. L.; Glickson, J. D. *J. Am. Chem. Soc.* **1979**, *101*, 3071–3077.

(49) The observed T_{1P}^{-1} for a given nucleus will be a mole-fraction weighted sum of T_1^{-1}'s for the different adducts when the τ_M's are small relative to the T_1's.

Table III. Proton NMR Data

		sample		
position	shift[a]	F	G	H[b]
Paramagnetic Contributions to Proton Spin–Lattice Relaxation Rates, T_{1P}^{-1}, s^{-1} [c]				
C(3)H	4.89	18.04 (150)	12.62 (32)	16.68 (109)
C(6)H$_2$	3.05	12.08 (32)	8.61 (19)	10.90 (20)
C(5)H$_3$	1.87	*d*	*d*	5.80 (18)
Distance Ratios[e]				
$r(3)/r(6)$		0.935 (17)	0.938 (7)	0.932 (13)
$r(3)/r(5)$		*d*	*d*	0.839 (13)
Comparison of Gd–Proton Distances,[f] Å				
Gd–C(6)H$_2$ NMR		5.61 (19)	5.60 (23)	5.63 (27)
X-ray		5.50 (25)	5.50 (25)	5.50 (25)
Gd–C(5)H$_3$ NMR		*d*	*d*	6.26 (31)
X-ray				6.54 (22)

[a] Chemical shift in ppm from Me$_4$Si. [b] Sample contains Eu(fod)$_3$ in addition to Gd(fod)$_3$ or La(fod)$_3$. [c] Observed relaxation rates less T_{1f}^{-1} and T_{1os}^{-1}. Rates observed in the presence of La(fod)$_3$ are 0.233 (4) and 0.729 (12) for C(3)H and C(6)H$_2$, respectively. Rates observed in the presence of La(fod)$_3$ *and* Eu(fod)$_3$ are 0.464 (14), 0.855 (53), and 0.729 (39) for C(3)H, C(6)H$_2$, and C(5)H$_3$, respectively. A correction of 0.16 s^{-1} for T_{1os}^{-1} was made in all cases. Sample temperature is 303 ± 1 K in all cases. Errors in the least significant digits are given in parentheses. [d] Data not available due to coincidence of C(1)H$_3$ and C(5)H$_3$ methyl resonances. [e] Ratios of distances from Gd to protons C(3)H and C(6)H$_2$ or C(5)H$_3$ determined from the NMR data. [f] NMR distances were determined by using the distance ratios and the Gd–C(3)H distance. "X-ray" distances were determined by using the experimental Gd coordinates found for sample A (Table II) and crystallographic coordinates for the protons nearest the Gd ion.

cyclohexane proton relaxation rates in a procedure analogous to that used for ^{13}C data. Differences in relaxation rates between diamagnetic and paramagnetic solutions were found to be 0.19 s^{-1} (Me$_4$Si) and 0.14 s^{-1} (cyclohexane). The T_{1P}^{-1} values shown for samples F and G in Table III are $T_{1\text{obsd}}^{-1}$ data less T_{1f}^{-1} and less an average estimated T_{1os}^{-1} of 0.16 s^{-1}. These T_{1P}^{-1} values were used to determine the Gd–proton distance ratios, $r(3)/r(6)$, shown in the table.

Comparison of Gd–proton distances determined by the T_1 experiments with values calculated from crystallographic coordinates is not as straightforward as was the case for carbons. The four ethylenic protons give only one resonance signal which apparently has a single time constant for spin–lattice relaxation. However in the instantaneous structure of the adduct there are four different Gd–proton distances for the ethylene bridge, if it retains the gauche conformation found in the solid state,[28] or two Gd–proton distances if the eclipsed conformation exists. A combination of several factors is believed to result in fast site exchange among the ethylenic protons: (1) Gd(fod)$_3$ can bind with equal probability on either side of the plane of I; (2) τ_M is short in comparison to T_1's; (3) the ethylene bridge probably undergoes rapid conformational changes.[50] The effective T_{1P}^{-1} for C(6)H$_2$ is thus a sum of T_{1P}^{-1}'s for all sites which, in turn, is proportional to the sum of r^{-6}'s. It is expected that the effective T_{1P}^{-1} will be dominated by contributions from the protons *nearest* Gd in the instantaneous structure due to the r^{-6} dependence. Assuming this, the "NMR" distance from Gd to the nearest axial C(6)–proton[51] was calculated by using the experimental $r(3)/r(6)$ values and $r(3)$ determined from crystallographic coordinates. The Gd position found for samples A (Table II) was used in the latter calculation. NMR and "X-ray" distances are compared in Table III, and it can be seen that the agreement is well within the limits of error.

In an effort to measure the methyl proton relaxation rates, Eu(fod)$_3$ was added to solutions of I which also contained Gd(fod)$_3$ or La(fod)$_3$. Isotropic shifts induced by Eu(fod)$_3$ separate the otherwise coincident methyl signals. Data thus obtained for C(3)H, C(6)H$_2$, and C(5)H$_3$ are given in column H of Table III. The signal from C(1)H$_3$ was extremely broad in these experiments, and accurate T_1 data could not be obtained. The $r(3)/r(5)$ ratio from the NMR data may be used, with $r(3)$ determined as above, to calculate an effective $r(5)$ value of 6.26 (31) Å. this may be compared with the value of 6.54 (22) Å calculated by using X-ray coordinates as described above.

Correlation Times. Approximate values for the effective correlation time, τ_c, of the adduct may now be calculated by using Gd–nuclear distances determined above. Equation 1 is used with the assumptions that $\omega_I^2\tau_c^2 << 1$ and $\omega_S^2\tau_c^2 >> 1$, and it is assumed that Gd is located at the coordinates found for sample A. When Gd–C(2) and Gd–C(3)H distances are used in the calculations, effective correlation times of $\sim 2 \times 10^{-11}$ s (sample A) and $\sim 6 \times 10^{-11}$ s (sample F), respectively, are found. These are smaller than expected for a molecule as large as the adduct II. The reported value for Gd(H$_2$O)$_n^{3+}$, for example, is 4.5×10^{-11} s.[52]

Another method of estimating effective τ_c's involves use of eq 6. T_1^{-1} is the contribution to the relaxation rate of a ^{13}C

$$T_1^{-1} = (n_H\gamma_H^2\gamma_C^2\hbar^2/r_{CH}^6)\tau_c \qquad (6)$$

nucleus due to dipolar interactions with n_H protons bound to the carbon at distance r_{CH}.[53] In substrate I, C(3) is expected to be a good probe of the motions of the molecular frame. The full NOE is found for C(3), demonstrating that observed relaxation rates are dominated by dipolar interactions with the proton. Using T_1 data for C(3) in a diamagnetic environment and assuming r_{CH} = 1.1 Å, one obtains a value of $\tau_c = 3.0 \times 10^{-11}$ s. This τ_c is for the free substrate I rather than for the adduct II. The *relative* reorientational correlation times of the adduct and substrate were estimated to be ~3:1 by using the Stokes–Einstein relationship and approximate molecular radii measured on scale models. This would imply that τ_c for the adduct is $\sim 9 \times 10^{-11}$ s.

Summary. The nickel(II) complex, I, binds via its oxygen atoms to Gd(fod)$_3$, forming an adduct, II, which has a short lifetime. Spin–lattice relaxation rates for C(1) and C(2) of I in the presence of Gd(fod)$_3$ are used to establish the position of bound Gd ion to within a few tenths of an ångstrom. The Gd ion is found to be ~1.8 Å out of the plane of I in the adduct.

Relaxation rate data for the other carbons and protons of I in the presence of Gd(fod)$_3$ are used to determine the corresponding Gd–nuclear distances. These agree within the limits of error with distances calculated by using crystallographic data for I and the Gd position from NMR data for C(1) and C(2). The best fit for the data is found for a Gd–O bond length of 2.45 Å.

---

(50) Rapid interconversion between gauche conformations is well-known in coordination compounds of ethylenediamine and its derivatives. Interconversion rates as large as 10^4 s^{-1} can be calculated by using estimated separations of axial and equatorial signals in paramagnetic complexes: Ho, F. F. L.; Reilley, C. N. *Anal. Chem.* **1969**, *41*, 1835–1841.

(51) Using crystallographic coordinates to determine relative r^{-6} values for the four ethylene protons in the gauche conformation, it is possible to show that the expected contribution to the effective T_{1P}^{-1} for the axial proton nearest Gd is about *twice* as great as that of any other proton.

(52) Dwek, R. A.; Richards, R. E.; Morallee, K. G.; Nieboer, E.; Williams, R. J. P.; Xavier, A. V. *Eur. J. Biochem.* **1971**, *21*, 204–209.

(53) Lyerla, J. R.; Levy, G. C. In "Topics in Carbon-13 NMR Spectroscopy"; Levy, G. C., Ed.; Wiley-Interscience: New York, 1974; Vol. I, Chapter 3.

The four methylene protons of I in the adduct undergo rapid site exchange. A single, effective T_1^{-1} is found which is dominated by the relaxation rate of the proton nearest Gd.

Acknowledgment. We thank the University of Kansas Computation Center for a generous allocation of computer time. The Bruker WP-80 spectrometer was purchased in part with an instrumentation grant from the National Science Foundation.

Registry No. I, 13878-48-3; Gd(fod)$_3$, 17631-67-3; La(fod)$_3$, 19106-89-9; Eu(fod)$_3$, 17631-68-4.

Contribution from the Department of Chemistry,
University of Windsor, Windsor, Ontario, Canada N9B 3P4

Gallium-71 NMR Studies of Anionic Gallium Halide Species in Nonaqueous Solution

BRUCE R. McGARVEY, MICHAEL J. TAYLOR, and DENNIS G. TUCK*

Received November 21, 1980

^{71}Ga NMR spectra of the four-coordinate anions $GaX_nY_{4-n}^-$ and GaX_2YZ^- (X, Y, Z = Cl, Br, or I) are reported. Halide exchange between GaX_4^- and GaY_4^- in dichloromethane solution is slow, and the equilibrium proportions of the mixed-halide species GaX_3Y^-, $GaX_2Y_2^-$, and $GaXY_3^-$ do not correspond to a statistical redistribution of ligands. No resonance was detected from solutions of salts of $Ga_2X_6^{2-}$ (X = Cl or Br), which have a staggered ethane-type structure.

Introduction

Gallium is known to form tetrahalogeno complexes of the formulas GaX_4^- (X = Cl, Br, I) and $GaX_nY_{4-n}^-$, and partial or complete vibrational spectra have been reported for both series of anions.[1-5] Recent papers from this laboratory have reported the preparation and spectroscopic investigation of the analogous $InX_nY_{4-n}^-$ species,[6] and the use of ^{115}In NMR spectroscopy[7] in the study of the solution chemistry of these and related anions.

The tetrahedral GaX_4^- ions have been studied by ^{71}Ga NMR spectroscopy, both in aqueous solution and in melts.[8] In general, the quadrupole of the ^{71}Ga nucleus ($I = {}^3/_2$) means that resonance can only be observed in structures of high symmetry[9] such as octahedral or tetrahedral complexes or in species in which the Ga^{3+} ion is bonded to chemically similar ligands and especially halides. ^{71}Ga inversion–recovery spectra from a solution of $GaBr_3$ and $NbCl_5$ in acetonitrile have been studied[10,11] and the five experimental peaks assigned to the series $GaCl_4^-$–$GaCl_nBr_{4-n}^-$–$GaBr_4^-$.

We have now carried out ^{71}Ga NMR studies of the anionic four-coordinate gallium(III) chloride, bromide, and iodide mixed-halide complexes in dichloromethane solution and have obtained chemical shifts and other data for all the possible four-coordinate species $GaX_nY_{4-n}^-$ and GaX_2YZ^- (where X, Y, Z = Cl, Br, or I). Complex ions of the type MX_2YZ^- have not been previously reported for gallium. A particularly interesting aspect of the results is that the ligand-exchange reactions between GaX_4^- and GaY_4^- are found to be slow, so that ^{71}Ga NMR spectroscopy is a convenient technique for following the progress of the formation of the mixed-halide complexes. The behavior of gallium complexes is in contrast to that of the corresponding four-coordinate indium species[7] under similar conditions, since the formation of the InX_3Y^- and $InX_2Y_2^-$ anions (X ≠ Y = Cl, Br, or I) is complete within the time of mixing, yielding the mixed-halide complexes in proportions corresponding approximately to the statistical redistribution of the ligands.

Table I. ^{71}Ga Resonances for $GaX_4Y_{4-n}^-$ and GaX_2YZ^- Anions in Dichloromethane

no.	anion	$-\delta$ (±1%)	$w_{1/2}$(±5%), Hz
1	$GaCl_4^-$	0	180
2	$GaCl_3Br^-$	40	200
3	$GaCl_2Br_2^-$	84	215
4	$GaClBr_3^-$	133	210
5	$GaBr_4^-$	187	185
6	$GaBr_3I^-$	300	205
7	$GaBr_2I_2^-$	425	220
8	$GaBrI_3^-$	561	210
9	GaI_4^-	706	185
10	$GaCl_3I^-$	128	220
11	$GaCl_2I_2^-$	291	320
12	$GaClI_3^-$	486	290
13	$GaCl_2BrI^-$	181	255
14	$GaClBr_2I^-$	238	290
15	$GaClBrI_2^-$	356	340

Experimental Section

Materials. The previously reported[12] gallium salts $(n\text{-}C_4H_9)_4NGaX_4$ were prepared by dissolving gallium metal in an aqueous solution of the acid HX, prepared by mixing the concentrated reagent with an equal volume of water. The solution was boiled to ensure oxidation of Ga(II) intermediates to Ga(III) before adding a slight excess of tetra-*n*-butylammonium halide. The precipitated $(n\text{-}C_4H_9)_4NGaX_4$ was collected, dried, and recrystallized from dichloromethane; addition of diethyl ether resulted in the product being recovered in the form of small crystals. The identity of the products was confirmed by infrared and Raman spectroscopy.

The gallium(II) salts $[(n\text{-}C_4H_9)_4N]_2[Ga_2X_6]$ (X = Cl, Br) were prepared by methods previously reported.[13]

Dichloromethane was dried and stored over molecular sieves.

NMR Spectroscopy. ^{71}Ga NMR spectra were obtained with a Bruker CXP-100 variable-frequency FT spectrometer operating at 27.45 MHz, with a magnetic field of 2.114 T. The instrument was

---

(1) Rafaeloff, R.; Silverstein-Hirsch, A. *Spectrochim. Acta, Part A* **1975**, *31A*, 183.
(2) Grigor'ev, A. N.; Grigor'ev, A. I.; Spiridonov, F. M.; Mikheeva, M.; Komissarova, L. N. *Russ. J. Inorg. Chem. (Engl. Transl.)* **1977**, *22*, 508.
(3) Woodward, L. A.; Nord, A. A. *J. Chem. Soc.* **1956**, 2655.
(4) Woodward, L. A.; Nord, A. A. *J. Chem. Soc.* **1956**, 3721.
(5) Woodward, L. A.; Singer, G. H. *J. Chem. Soc.* **1958**, 716.
(6) Drake, J. E.; Hencher, J. L.; Khasrou, L. N.; Tuck, D. G.; Victoriano, L. *Inorg. Chem.* **1980**, *19*, 34.
(7) McGarvey, B. R.; Trudell, C. O.; Tuck, D. G.; Victoriano, L. *Inorg. Chem.* **1980**, *19*, 3432.
(8) Akitt, J. W.; Greenwood, N. N.; Storr, A. *J. Chem. Soc.* **1965**, 4410.
(9) Hinton, J. F.; Briggs, R. W. In "NMR and the Periodic Table"; Harris, R. K., Mann, B. E., Eds.; Academic Press: London, 1978; pp 285–286.
(10) Tarasov, V. P.; Privalov, V. I.; Buslaev, Yu. A.; Kuzmin, I. A. *Dokl. Akad. Nauk* **1977**, *234*, 636.
(11) Wehrli, F. W. *Annu. Rep. NMR Spectrosc.* **1979**, *9*, 125.
(12) Carty, A. J. *Coord. Chem. Rev.* **1969**, *4*, 29.
(13) Evans, C. A.; Tan, K.-H.; Tapper, S. P.; Taylor, M. J. *J. Chem. Soc., Dalton Trans.* **1973**, 988.